

## Enhanced orbital magnetism at the nanostructured Co/Cu(1 1 13) surface

H. A. Dürr and G. van der Laan

*Daresbury Laboratory, Warrington WA4 4AD, United Kingdom*

J. Vogel

*Laboratoire de Magnetisme Louis Néel, CNRS, F-38043 Grenoble, France*

G. Panaccione

*LURE, CNRS-CEA-MEN, F-91405 Orsay, France*

*and Institut de Physique, Université Neuchâtel, CH-2000 Neuchâtel, Switzerland*

N. B. Brookes

*ESRF, BP 220, F-38043 Grenoble, France*

E. Dudzik

*Daresbury Laboratory, Warrington WA4 4AD, United Kingdom*

*and Surface Science, University of Liverpool, Liverpool L69 3BX, United Kingdom*

R. McGrath

*Surface Science, University of Liverpool, Liverpool L69 3BX, United Kingdom*

(Received 22 July 1998)

Epitaxial growth of cobalt on a stepped copper surface leads to thin films displaying unusual electronic and magnetic properties. Strong changes in  $3d$  electron localization near the surface of the Co film augment the ground-state energy compared to the bulk of the film. The Co orbital magnetic moment per spin is separated into bulk and surface contributions using magnetic circular x-ray dichroism. Symmetry breaking due to finite size effects results in an increase (200%) of the orbital moment near the surface. [S0163-1829(98)50342-6]

The reduced dimensionality at solid surfaces can result in a variety of unusual electronic<sup>1</sup> and magnetic<sup>2</sup> properties absent in bulk materials. Metallic systems have a tendency to respond to the reduction of atomic coordination with a smoothening of the surface charge corrugation that tries to restore a *bulklike* surface electronic structure. Interesting fundamental and applied systems of growing technological relevance for magnetic information storage devices are those where the surface electronic and magnetic structure can be tailored to mimic a wider range of materials spanning from itinerant  $3d$  metals to localized lanthanides and actinides. It is often the modified electronic structure at the surface which determines the magnetic properties of the underlying substrate.<sup>2,3</sup>

In this respect, the orbital moment provides a direct link between electronic structure and the magnetocrystalline anisotropy, determining the preferred spin orientation direction.<sup>4,5</sup> In an ionic compound the orbital moment originates from the spin-orbit coupling and can reach large values, theoretically up to  $3\mu_B$  for Co. In metallic bulk fcc Co this orbital moment is reduced to  $0.078\mu_B$  by the strong crystalline field interaction.<sup>6</sup> However, hybridization<sup>7</sup> as well as localization<sup>6</sup> of  $3d$  electrons at the interface or surface can increase this value. It has recently been demonstrated that in magnetic materials with more than half-filled  $d$  shells the spins have a preference to orient along the crystalline axis with the largest orbital moment expectation value,<sup>8,9</sup> thereby fixing the easy direction of magnetization. It is expected that

even tiny changes in the surface or interface orbital moment can have a dramatic effect on the magnetic anisotropy of the system over a large scale.

In this paper we describe a system, Co films grown epitaxially on a stepped Cu(1 1 13) surface, that displays several interesting features. The unusual characteristics of a surface layer with a strongly localized electronic structure on top of an itinerant Co metal substrate is manifest in a significantly different ground-state energy for bulk and surface which results in a surface core-level shift in x-ray absorption spectroscopy (XAS) of a metallic system. The observed electron localization is a direct consequence of the electron confinement at the nanostructured surface and results in a giant increase (200%) of the surface orbital magnetic moment compared to the bulk of the Co film. It also leads to a dramatically different  $3d$ -band filling. None of these features have been observed in Co films grown on a planar Cu(001) surface where the Co film surface is simply a truncation of the bulk structure resulting in a surface orbital moment enhancement of only 40%.<sup>6</sup> This highlights the importance of a laterally nanostructured surface morphology and has important implications for interfaces where nanostructuring could also significantly contribute to the reported orbital moment enhancements such as for the Co/Pd interface (100%).<sup>7</sup> Our observation of a giant surface orbital moment also offers a microscopic explanation for the magnetic switching phenomena which depend on the surface modification as reported for Co films grown on vicinal Cu(001) substrates.<sup>2</sup>

The Cu(1113) single crystal substrate was prepared under ultrahigh vacuum conditions by cycles of Ne ion bombardment and annealing to 700 K. Co was deposited at a pressure of  $1 \times 10^{-10}$  mbar and the thickness was determined by a quartz microbalance. All Co depositions and subsequent measurements presented here were done at room temperature. Auger electron spectroscopy (AES) and x-ray photoelectron spectroscopy (XPS) gave no evidence of Cu segregation to the film surface. Contamination levels of the films were below the detection limit of AES and XPS. XAS at the Co  $2p$  absorption edges was performed with a photon energy resolution of 200 meV at beamline ID12B of the European Synchrotron Radiation Facility in Grenoble by monitoring the total electron yield. The photon energy could be set reproducibly with an accuracy of 10 meV. Magnetic circular x-ray dichroism (MCXD) measurements were performed by reversing the helicity of 85% circularly polarized x rays incident at  $30^\circ$  relative to the surface along the easy magnetization direction (parallel to the surface steps).<sup>10</sup> The as-grown films were found to be remanently magnetized by residual magnetic fields.

Surface crystallinity and morphology were monitored with high-resolution low-energy electron diffraction which will be presented in detail elsewhere<sup>11</sup> and is summarized only briefly here. The Cu(1113) surface is characterized by a regular staircaselike structure with 17 Å-wide (001) terraces separated by monatomic steps along the close-packed [110] lattice direction. The straight steps on the clean substrate were found to roughen upon Co deposition in agreement with previous scanning tunneling microscopy measurements on other vicinal Cu(001) surfaces.<sup>12</sup> This reduces the effective terrace size parallel to the steps. We found good lateral epitaxy of Co. The in-plane Co lattice parameter was equal to that of the Cu substrate within  $\pm 0.3\%$  up to  $\sim 15$  monolayers (ML). Between 15 and 20 ML the Co lattice was found to contract slightly perpendicular to the steps by 0.5% relative to the substrate atomic spacing. This indicates a partial relaxation of the lattice strain caused by the  $\sim 2\%$  lattice mismatch of fcc Co and Cu.<sup>13</sup> We will show below how this particular surface morphology affects the electronic and magnetic surface properties.

XAS was employed as an element-specific tool to study the  $3d$  electronic structure of Co. At the spin-orbit split  $L_3(2p_{3/2})$  and  $L_2(2p_{1/2})$  edges in XAS,  $2p$  electrons are excited into unoccupied  $3d$  and continuum states which give rise to the peaks and the background modeled by the step function in Fig. 1. Typical measured XAS spectra are shown for 2.5 ML (lines and symbols) and 28 ML (lines) Co coverage. While there is hardly any change at the  $L_2$  edge, it is clear that the  $L_3$  absorption structure consists of at least two distinct contributions: a peak  $S$ , dominant at low coverages which decreases in intensity with increasing film thickness, and a peak  $B$ , which dominates for thicker films. Peak  $S$  remains roughly at the same energy position and is still discernible as a weak shoulder at higher coverages (see insets in Fig. 1). We assign peak  $S$  to a surface feature whereas peak  $B$  reflects transitions into unoccupied  $3d$  states mainly localized in the bulk of the Co film.

The final state of XAS contains an extra  $3d$  electron compared to the ground state which effectively screens the  $2p$  core hole.<sup>14</sup> XAS is, therefore, in contrast to XPS very sen-

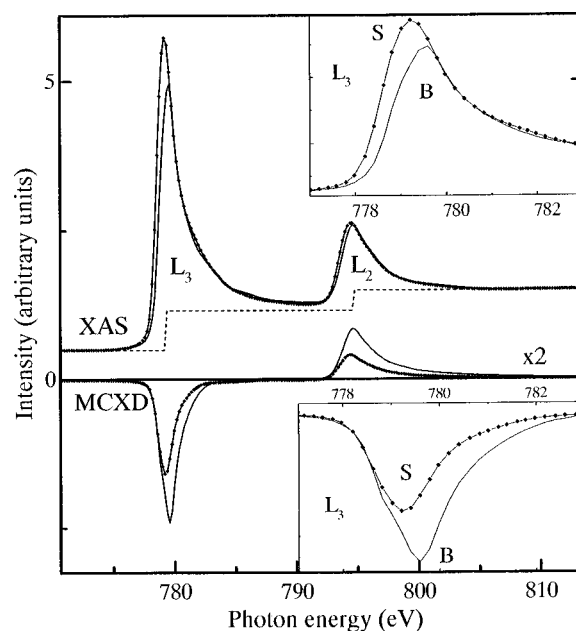


FIG. 1. Sum (XAS) and difference (MCXD) spectra for 2.5 ML (drawn lines with symbols) and 28 ML (drawn lines) Co coverage. The XAS spectra were normalized to a constant edge jump which models the excitations into continuum states (dashed line). Top inset: XAS  $L_3$  absorption edge enlarged. Bottom inset: MCXD  $L_3$  absorption edge enlarged. Surface  $S$  and bulk  $B$  contributions to the XAS and MCXD spectra are indicated.

sitive to changes in the ground-state energy induced by a different atomic coordination or local chemical environment. The energy separation between peaks  $S$  and  $B$  of  $\sim 0.5$  eV points, therefore, to a drastically different ground-state energy for surface atoms. When the Co thickness is varied the atomic surrounding changes from isolated atoms at submonolayer coverages to mainly a bulk coordination for thick films. This leads to the photon energy shifts observed for the intensity maxima at the  $L_{2,3}$  structures shown in Fig. 2. The large energy shift of the  $L_3$  edge up to 3 ML reflects the intensity transfer from peak  $S$  to peak  $B$  and indicates a rapid increase in atomic coordination. This coverage also corre-

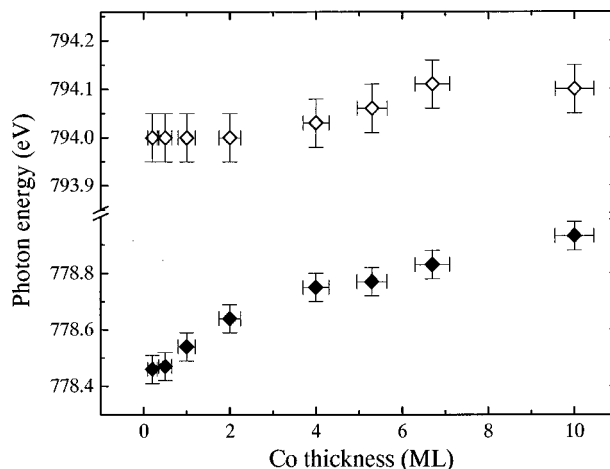


FIG. 2. Photon energy of the XAS peak maxima at the  $L_3$  (solid symbols) and  $L_2$  (open symbols) edges (cf. Fig. 1) versus Co film thickness.

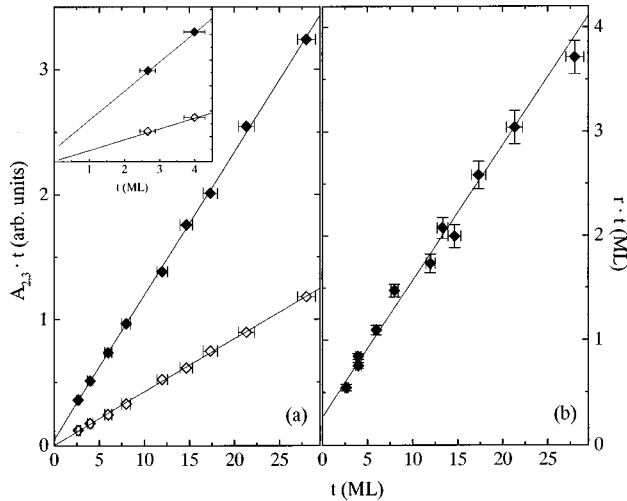


FIG. 3. (a) Integrated XAS area at the  $L_3$  (solid symbols) and  $L_2$  (open symbols) edges corrected with the step function (dashed line in Fig. 1) and (b) orbital moment per spin  $r$ , as determined by applying sum rules<sup>18</sup> to the integrated areas at the  $L_3$  and  $L_2$  edges of the MCXD spectra (cf. Fig. 1) times Co film thickness  $t$ , versus  $t$ . Vertical error bars in (a) are given by the symbol size. The drawn lines represent linear fits to the error weighted data. The inset shows the enlarged low-coverage region in (a).

sponds to the onset of a smaller shift at the  $L_2$  structure where peak  $S$  is absent. For thicker films the surface signal  $S$  is still visible (Fig. 1) but is diluted by the bulk of the Co film underneath due to the relatively large XAS sampling depth of  $\sim 10$  ML.<sup>15</sup> Note that the observed break point at 3 ML in Fig. 2 occurs at twice the coverage of Ni/Cu(001) films<sup>16</sup> which indicates that the ground-state energy of more than only the Co surface layer is altered.

To quantify the difference in surface and bulk electronic structure we studied the integrated XAS signals  $A_{2,3}$  of the  $L_{2,3}$  edges corrected for transitions into continuum states (dashed line in Fig. 1) and saturation.<sup>6,8</sup> The total area is proportional to the number of  $3d$  holes  $n_h \propto A_3 + A_2$  in the ground state.<sup>17</sup> Figure 3(a) shows  $A_{2,3}$  multiplied by the Co film thickness  $t$  versus  $t$ . With the XAS spectra normalized to a constant edge jump as shown in Fig. 1, all quantities obtained are given per Co ML. The value of  $A_{2,3}t$  increases, therefore, linearly in  $t$  with a slope given by  $A_{2,3}$  of the bulk of the film. The vertical offset at  $t=0$  ML determines the surface enhancements of  $A_{2,3}$ . From a linear fit to the error weighted data, we obtain an increase in  $n_h$  of  $0.7 \pm 0.2$  holes at the surface, assuming for the bulk of the film a value of 2.4 holes which would be the bulk fcc Co value.<sup>9</sup> The determined surface enhancement of  $n_h$  is clearly outside the statistical error. Interestingly no similar increase was observed for Co/Cu(001).<sup>6</sup> Figure 3(a) also shows that only  $A_3$  is enhanced at the surface while  $A_2$  has roughly the same value for bulk and surface. This can be quantified by the branching ratio  $B_r = A_3 / (A_3 + A_2)$ . We obtain a bulk value of  $B_r = 0.73 \pm 0.01$  and a surface increase of  $10 \pm 7\%$  relative to the bulk. Since  $B_r$  for Co metal is mainly influenced by the spin-orbit expectation value per hole  $\langle l \cdot s \rangle / n_h$  in the ground state<sup>17</sup> our measurements indicate an enhanced surface value of  $\langle l \cdot s \rangle / n_h$ .

The strong difference between bulk and surface seen in XAS is expected to give a dramatic change in the associated

magnetic moments. The latter can be determined by MCXD which utilizes the different XAS signals depending on the (anti)parallel alignment of photon helicity and sample magnetization. Using the sum rules for the integrated MCXD signals ( $\Delta A_{2,3}$ ) at the  $L_{2,3}$  edges, orbital ( $m_L = -L_z \mu_B$ ) and spin ( $m_S = -2S_z \mu_B$ ) magnetic moments can be separated.<sup>18</sup>  $L_z$  and  $S_z$  are the expectation values of orbital and spin moments, respectively, along the sample magnetization direction. The MCXD spectra in Fig. 1 display the same peaks  $S$  and  $B$  as the corresponding XAS spectra. The smaller signal for the 2.5 ML MCXD spectrum is caused by a lower ordering temperature compared to the thicker films. This makes it difficult to obtain absolute moments, but we can still find the orbital magnetic moment per spin,  $r \equiv m_L / (m_S + m_T) = \frac{2}{3} (\Delta A_3 + \Delta A_2) / (\Delta A_3 - 2\Delta A_2)$ .<sup>6,19</sup> The magnetic dipole term  $m_T$ , which is usually less than 20% of  $m_S$  (Refs. 6, 8, and 19) will be neglected in the following. From the linear fit to the error weighted data  $r \cdot t$  versus  $t$  [Fig. 3(b)] we obtain the bulk contribution as  $r_{\text{bulk}} = 0.13 \pm 0.01$  per Co ML and a surface increase of  $\Delta r_{\text{surface}} = 0.26 \pm 0.04$ . We note that due to the MCXD mean probing depth of about 10 ML,<sup>6,15</sup> for lower coverages we cannot differentiate whether  $\Delta r_{\text{surface}}$  is indeed caused by the surface or by the Co/Cu interface. However, from the fit above  $t=10$  ML we obtain a similar value for  $\Delta r_{\text{surface}}$  which proves its connection to the Co film surface.

It is instructive to compare these values of  $r$  with results for Co films grown on a planar Cu(001) surface.<sup>6</sup> Our value of  $r_{\text{bulk}}$  shows a 60% increase compared to that for Co/Cu(001).<sup>6</sup> The reason might be a somewhat larger lattice disorder for the Co/Cu(1 1 13) system due to a possibly distorted epitaxy at the Cu step edges. While for Co/Cu(001) a  $\sim 40\%$  increase of the surface orbital moment relative to the bulk of the film was reported,<sup>6</sup> the increase in our case is 200%. Such a large value for the surface orbital moment exceeds any reported value to date<sup>6</sup> and indicates very clearly the existence of a different modification of Co in the surface region.

The observed surface enhancements demonstrate a significantly different magnetic ground state compared to the bulk of the Co/Cu(1 1 13) film or the Cu/Cu(001) system. A reduced electronic hopping between sites at the surface is reflected in the narrowing of the  $3d$  bandwidth.<sup>6,20</sup> The increase in the number of  $3d$  holes at the surface, observed in our experiments and predicted theoretically,<sup>20</sup> can then be accommodated by a shift of the  $3d$ -band center towards the Fermi level,  $E_F$ . In a simple one-electron picture which assumes a constant  $3d$ - $2p$  energy separation, the  $2p$  core level will also be shifted at the surface.  $E_F$  then intersects the bulk and surface  $3d$  bands at different energies relative to the band centers which leads to the observed difference in XAS excitation energy for peaks  $S$  and  $B$  into the unoccupied valence states for surface and bulk Co.

We assign the giant orbital moment enhancement along the step edges as the driving force<sup>4,5,8,9</sup> for the large uniaxial magnetic anisotropy observed for Co/Cu(1 1 13).<sup>10</sup> A strongly anisotropic electronic structure localized at the step-edge atoms as was originally suggested<sup>2</sup> can be ruled out. The low density of these sites would require a local orbital moment close to  $2\mu_B$  to produce the observed effect, which is unreasonable. Also the observed increase for the value of

3d holes at the surface is too large to be accommodated in only one Co surface layer. Our results demonstrate that the electron localization must be spread out over several surface layers. The structural cause for this behavior is unlikely to be due to an anomalous lattice distortion, as we find a lateral strain relaxation with increasing thickness which does not seem to affect the electronic and magnetic surface properties. A similar strain relaxation occurs for the Co/Cu(001) system around 10 ML (Ref. 13) without a corresponding huge orbital moment enhancement.<sup>6</sup> It is more likely that the nanostructured surface morphology plays a dominant role, since the observed phenomena are clearly absent for planar Co films.<sup>6</sup> It has been shown that electronic surface states can be confined on small terraces leading to changes in the elec-

tronic structure analogous to quantum well states.<sup>21</sup> Step edges can furthermore influence the electronic and magnetic structure of several layers below<sup>22</sup> which might result in increased electron confinement on the terraces even below the surface layer. Adsorption at the steps can then alter this electron confinement and influence the magnetic anisotropy of the film as observed in Ref. 2 through changes in the surface orbital moment. It will be interesting to see first-principles calculations which are able to describe Co/Cu(001) correctly<sup>19</sup> and which are starting to become feasible even for the stepped surfaces.

We thank K. Larsson for his help and technical assistance and the ESRF staff for the excellent operation conditions.

- 
- <sup>1</sup>P. T. Sprunger *et al.*, *Science* **275**, 1764 (1997).  
<sup>2</sup>W. Weber *et al.*, *Nature (London)* **374**, 788 (1995).  
<sup>3</sup>G. H. O. Daalderop, P. J. Kelly, and M. F. H. Schuurmans, in *Ultrathin Magnetic Structures*, edited by J. A. C. Bland and B. Heinrich (Springer, Berlin, 1994).  
<sup>4</sup>J. Stöhr and H. König, *Phys. Rev. Lett.* **75**, 3748 (1995).  
<sup>5</sup>H. A. Dürr and G. van der Laan, *Phys. Rev. B* **54**, R760 (1996).  
<sup>6</sup>M. Tischer *et al.*, *Phys. Rev. Lett.* **75**, 1602 (1995).  
<sup>7</sup>D. Weller *et al.*, *Phys. Rev. B* **49**, 12 888 (1994).  
<sup>8</sup>D. Weller *et al.*, *Phys. Rev. Lett.* **75**, 3752 (1995).  
<sup>9</sup>H. A. Dürr *et al.*, *Science* **277**, 213 (1997).  
<sup>10</sup>A. Berger, U. Linke, and H. P. Oepen, *Phys. Rev. Lett.* **68**, 839 (1992).  
<sup>11</sup>H. A. Dürr *et al.* (unpublished).  
<sup>12</sup>M. Giesen, F. Schmitz, and H. Ibach, *Surf. Sci.* **336**, 269 (1995).  
<sup>13</sup>E. Navas *et al.*, *J. Magn. Magn. Mater.* **121**, 65 (1993).  
<sup>14</sup>O. Gunnarsson and K. Schönhammer, *Phys. Rev. B* **38**, 3158 (1988).  
<sup>15</sup>W. L. O'Brien and B. P. Tonner, *Phys. Rev. B* **50**, 12 672 (1994).  
<sup>16</sup>B. Hernäs *et al.*, *Surf. Sci.* **302**, 64 (1994).  
<sup>17</sup>B. T. Thole and G. van der Laan, *Phys. Rev. B* **38**, 3158 (1988).  
<sup>18</sup>B. T. Thole *et al.*, *Phys. Rev. Lett.* **68**, 1943 (1992); P. Carra *et al.*, *ibid.* **70**, 694 (1993).  
<sup>19</sup>O. Hjortstam *et al.*, *Phys. Rev. B* **53**, 9204 (1996).  
<sup>20</sup>R. Wu and A. J. Freeman, *Phys. Rev. Lett.* **73**, 1994 (1994).  
<sup>21</sup>R. Fischer, Th. Fauster, and W. Steinmann, *Phys. Rev. B* **48**, R15 496 (1993).  
<sup>22</sup>A. V. Smirnov and A. M. Braikovsky, *Phys. Rev. B* **55**, 14 434 (1997).